Volume 25
Number 7
March 26, 1986

Inorganic Chemistry

Articles

Contribution from the Department of Chemistry,
University of Leuven, Celestijnenlaan 200F, 3030 Heverlee-Leuven, Belgium

Comparative Study of $Co(CN)_6^{3-}$ and $Co(CN)_5(OH)^{3-}$. Ab Initio Analysis of Ligand Substitution Effects

L. G. Vanquickenborne,* M. Hendrickx, I. Hyla-Kryspin, and L. Haspeslagh

Received March 7, 1985

The effect of ligand substitution in transition-metal complexes has been analyzed by means of a Hartree–Fock comparison between $Co(CN)_6^{3-}$ and $Co(CN)_5(OH)^{3-}$. The experimental ligand field spectrum is reasonably well predicted by SCF calculations. The sign of certain energy splittings is sometimes at variance with classical ligand field theory, but the general features of the metal–ligand interactions are found to be as expected from semiempirical considerations: the CN^- ligand behaves as a strong σ donor and weak π acceptor and the OH^- ligand as a weaker σ donor and as a π donor. This conclusion follows both from the analysis of the SCF excited energies and from the analysis of the density shifts; it does *not* follow from the relative order of the orbital energies in the ground state. To some extent, the postulate of ligand additivity is found to be substantiated by the ab initio calculations. This conclusion follows in part from energy considerations and especially from electron density considerations. In our Hartree–Fock treatment, the bond labilization induced by photoexcitation can be rationalized somewhat similarly as in simple ligand field theory: ^3E_a is characterized by axial labilization, whereas $^3A_2$ is characterized by equatorial labilization.

I. Introduction

Many of the most detailed SCF calculations on transition-metal complexes have been carried out for molecules of high symmetry. Indeed, for O_h, T_d, D_{4h}, ... systems, the number of integrals and the size of the matrices are reduced drastically when compared with those of equielectronic low-symmetry species. Near-Hartree–Fock-limit results have been obtained for molecules such as NiF_6^{4-}, $Cr(CN)_6^{3-}$, $Co(CN)_6^{3-}$, $Cr(CO)_6$, and many others.[1-5]

In the present work, we intend to study the influence of ligand substitution on the electronic structure of a high-symmetry complex. Whereas substitution effects can be handled quite readily by ligand field models, the ab initio treatment of this phenomenon represents a much more difficult problem. Approximate calculations in this direction have been carried out by Tennyson and Murrell[6] (minimal basis valence-electron approximation) and by Goursot and Pĕnigault[7] (multiple-scattering $X\alpha$ calculation). In what follows, we present a near-Hartree–Fock-limit comparison of $Co(CN)_6^{3-}$ and $Co(CN)_5(OH)^{3-}$. Apart from the inherent importance of the study of substitution effects at this level of approximation, the results should be able to throw some light on the mechanism of substitution reactions. Indeed, experimental data are available on both the thermal and photochemical reactions of $Co(CN)_5(OH)^{3-}$. In the thermal reaction, no CN^- release is observed, whereas the OH^- ligand can be replaced by other anions.[8] In the photochemical reaction, on the other hand, the quantum yield of CN^- release is quite significant; the OH^- quantum yield is not directly observable.[9] Although these facts can be rationalized quite readily in the framework of ligand field theory,[10,11] so far a discussion at the Hartree–Fock level has been lacking.

II. Method of Calculation

All calculations were carried out in the RHF–Roothaan formalism for open or closed shells, depending on the specific state under consideration. The orbital degeneracies, corresponding with the molecular symmetry, were obtained either by using the coupling coefficients describing the relevant open-shell states or else by an appropriate averaging of the different Fock matrix elements over the degenerate components of a given state.[2]

For the Co metal ion, we used the rather large (15s, 11p, 6d/11s, 8p, 4d) basis set, where the exponents and the contraction scheme were obtained by the procedure specified in two previous papers;[2,4] for the C, N, and O ligand atoms, we adopted the (9s, 5p/5s, 3p) bases proposed by Huzinaga and Dunning.[12]

(1) Wachters, A. J. H.; Nieuwpoort, W. C. *Phys. Rev. B: Solid State* **1972**, *5*, 291.
(2) Vanquickenborne, L. G.; Haspeslagh, L.; Hendrickx, M.; Verhulst, J. *Inorg. Chem.* **1984**, *23*, 1677.
(3) Sano, M.; Hatano, Y.; Kashiwagi, H.; Yamatera, H. *Bull. Chem. Soc. Jpn.* **1981**, *54*, 1523.
(4) Vanquickenborne, L. G.; Verhulst, J. *J. Am. Chem. Soc.* **1983**, *105*, 1769.
(5) Spangler, D. Wendoloski, J. J.; Dupuis, M.; Chen, M. M. L.; Schaefer, H. F. *J. Am. Chem. Soc.* **1981**, *103*, 3985.
(6) Tennyson, J.; Murrell, J. N. *J. Chem. Soc., Dalton Trans.* **1980**, 2395.
(7) Goursot, A.; Pĕnigault, E. *Chem. Phys.* **1981**, *61*, 83.
(8) Haim, A.; Wilmarth, W. K. *Inorg. Chem.* **1963**, *1*, 573. Burnett, A. G.; Gilfillan, W. M. *J. Chem. Soc., Dalton Trans.* **1981**, 1578.
(9) Wrighton, M.; Bredesen, D. *Inorg. Chem.* **1973**, *12*, 1707.
(10) Vanquickenborne, L. G.; Ceulemans, A. *J. Am. Chem. Soc.* **1977** *99*, 2208.
(11) Vanquickenborne, L. G; Ceulemans, A. *Coord. Chem. Rev.* **1983**, *48*, 157.
(12) Dunning, T. H. *J. Chem. Phys.* **1970**, *53*, 2823. Huzinaga, S. *J. Chem. Phys.* **1965**, *42*, 1293.

0020-1669/86/1325-0885$01.50/0

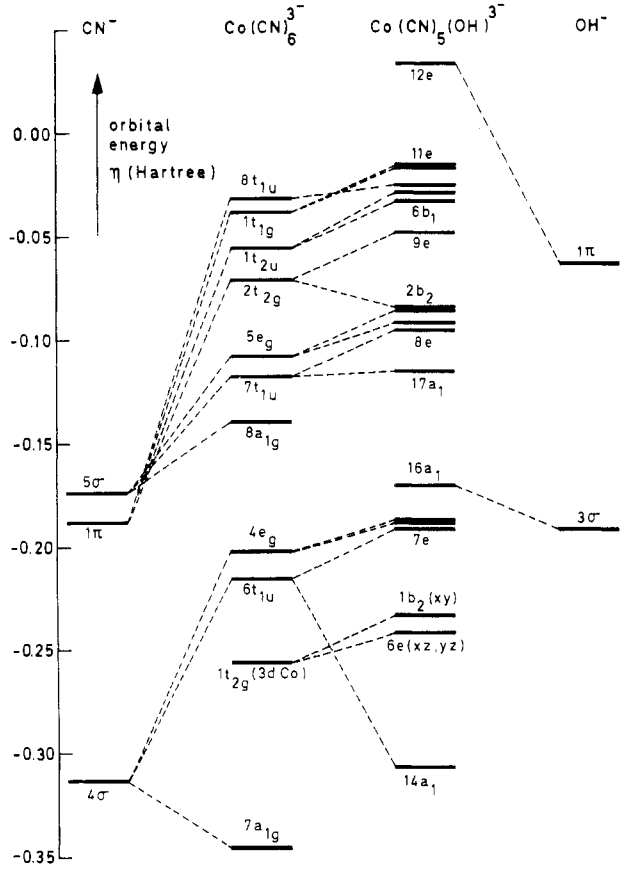

Figure 1. Orbital energy level diagram for the ground states $^1A_{1g}$ of $Co(CN)_6^{3-}$, and $^1A_1$ or $Co(CN)_5(OH)^{3-}$. The dashed lines connect orbitals of similar character in the metal complexes and in the individual ligands CN^- and OH^-.

The calculations for the hexacyano complex were carried out at the experimental bond lengths[13] R(Co–C) = 1.89 Å and R(C–N) = 1.15 Å. For the pentacyano complex no experimental distances have been published; therefore, the Co–C and C–N distances were taken identical with those in the hexacyano complex. No direct experimental evidence appears to be available on cobalt hydroxyl structures. In general,[14] the atomic radius of O is some 0.1 Å smaller than the atomic radius of C, suggesting a Co–O bond length of about 1.79 Å. But considering also the average Co–O distance in a number of polynuclear (oxygen-bridged) compounds,[15] we estimated[16] the Co–O distance in the present complex at 1.85 Å; the O–H distance was set equal to 0.97 Å, the average value in a series of hydroxo–metal compounds.

III. Description of the Ground States

1. Energy Considerations. The most important numerical information on the closed-shell ground states of the two complexes $Co(CN)_6^{3-}$ and $Co(CN)_5(OH)^{3-}$ is summarized in Table I and in Figure 1. The total energy of the $Co(CN)_6^{3-}$ ground state $^1A_{1g}$ is found at −1934.8834 hartree, which is approximately 0.5 hartree lower than the best calculations reported by Sano et al.[3,17] The improvement is obviously connected to the increased size and flexibility of the basis set. The order of the orbitals in the hexacyano complex is identical with the order given by Sano et al.,[17] and the orbital energies are quite similar. The orbital levels of the monohydroxo–pentacyano complex (C_{4v}) are connected to those of the parent octahedral (O_h) complex in the correlation diagram of Figure 1. In the setup of this diagram, only the dominant features of the orbitals were considered: each C_{4v} orbital is connected either to an O_h orbital or to an OH^- orbital. Indeed, in the C_{4v} complex, the hydroxyl orbitals are rather well preserved (OH^- character of ±80%); otherwise the general features of the orbitals of the substituted complex are essentially the same as in the parent octahedral compound. The $1t_{2g}$ orbitals and the corresponding 6e and $1b_2$ orbitals have approximately 92% 3dπ-(Co) character. The tetragonal splitting between $6e(d_{xz},d_{yz})$ and $1b_2(d_{xy})$ amounts to 1953 cm^{-1}, 6e being the more stable level. From ligand field theory, one would expect the opposite situation: since the OH^- ligand is generally considered to be the stronger π donor, the d_{xz},d_{yz} orbitals are expected to be more destabilized than d_{xy}. It is well to stress however that the orbital energy does not have the same meaning in ligand field theory as it has in SCF theory;[2] therefore, there is no real contradiction. This point will be reexamined in section IV.1, where the excited states are discussed.

It should also be noted that the Hartree–Fock d-type orbitals are definitely more ionic than either the Xα orbitals[7,18] or the

Table I. Total Energy E and Energy of the Topmost (Fully Occupied) Orbitals, η, of the Ground States of $Co(CN)_6^{3-}$ and $Co(CN)_5(OH)^{3-}$ (of $^1A_{1g}$ and $^1A_1$ Symmetry, Respectively)[a]

$Co(CN)_6^{3-}$ ($^1A_{1g}$) E = −1934.8834		$Co(CN)_5(OH)^{3-}$ ($^1A_1$) E = −1917.9725	
		$12e[\pi(OH)]$	+0.0345
$8t_{1u}[\pi(CN)]$	−0.0310		
		$11e[\pi(CN)]$	−0.0146
$1t_{1g}[\pi(CN)]$	−0.0376		
		$1a_2[\pi_{\parallel}(CN)_{eq}]$	−0.0157
		$19a_1[\pi_{\perp}(CN)_{eq}]$	−0.0244
		$10e[\pi(CN)]$	−0.0284
$1t_{2u}[\pi(CN)]$	−0.0550		
		$6b_1[\pi_{\perp}(CN)_{eq}]$	−0.0318
		$9e[\pi(CN)_{ax};\pi_{\perp}(CN)_{eq}]$	−0.0474
$2t_{2g}[\pi(CN)]$	−0.0706		
		$2b_2[\pi_{\parallel}(CN)_{eq}]$	−0.0845
		$5b_1[5\sigma(CN)_{eq}]$	−0.0849
$5e_g[5\sigma(CN)]$	−0.1075		
		$18a_1[5\sigma(CN)_{ax}]$	−0.0916
		$8e[5\sigma(CN)_{eq}]$	−0.0948
$7t_{1u}[5\sigma(CN)]$	−0.1172		
		$17a_1[5\sigma(CN)_{eq}]$	−0.1149
$8a_{1g}[5\sigma(CN)]$	−0.1386	$16a_1[3\sigma(OH)]$	−0.1701
		$4b_1[4\sigma(CN)_{eq}]$	−0.1873
$4e_g[4\sigma(CN)]$	−0.2017		
		$15a_1[4\sigma(CN)_{ax}]$	−0.1879
		$7e[4\sigma(CN)_{eq}]$	−0.1913
$6t_{1u}[4\sigma(CN)]$	−0.2154		
		$1b_2[3d_{xy}(Co)]$	−0.2332
$1t_{2g}[3d\pi(Co)]$	−0.2556		
		$6e[3d_{xz},3d_{yz}(Co)]$	−0.2421
		$14a_1[4\sigma(CN)_{eq}]$	−0.3069
$7a_{1g}[4\sigma(CN)]$	−0.3456		

[a] All energies are in hartrees. The dominant character of the orbitals is shown in brackets. As usual, in the pentacyano complex, the z axis is the heteroaxis, containing the hydroxyl ligand. The subscript ax refers to the axial ligands (on the z axis); the subscript eq refers to the equatorial ligands (in the xy plane). The notation $\pi_{\perp}$ and $\pi_{\parallel}$ designates ligand π orbitals having their nodal plane perpendicular or parallel to the z axis. The parentage designations 4σ(CN) and 5σ(CN) are only approximate: the ligand 4σ and 5σ orbitals are partly mixed by the octahedral field. In-phase mixing, of the type 4σ + 5σ, shifts electron density from C onto N, whereas out-of-phase mixing, of the type 4σ − 5σ, shifts electron density from N onto C. An example of the first type of complex orbital is $8a_{1g}$ (O_h); an example of the second type is $7a_{1g}$ (O_h).

(13) Vannerberg, N. *Acta Chem. Scand.* **1972**, *26*, 2863. Iwata, M.; Saito, Y. *Acta Crystallogr., Sect. B: Struct. Crystallogr. Cryst. Chem.* **1973**, *B29*, 82.
(14) Slater, J. C. "Quantum Theory of Molecules and Solids"; McGraw-Hill: New York, 1965; Vol. 2.
(15) Sim, G. A.; Sutton, L. E. "Molecular Structure by Diffraction Methods"; The Chemical Society: London, Vol. 2, 1974. *Ibid.*, Vol. 3, 1975.
(16) In ref 7, the Co–O distance was optimized at 2.04 Å by means of a series of Xα calculations. It is our experience, however, that distance optimalization of negative complexes tends to overestimate the metal–ligand distance. Also the comparison with the experimental Co–O distance (2.09 Å) in hydrated Co^{3+} appears less appropriate since the bonding properties of OH^- and H_2O are well-known[11] to be quite different.
(17) Sano, M.; Yamatera, H.; Hatano, Y. *Chem. Phys. Lett.* **1979**, *60*, 257.
(18) Goursot, A.; Pénigault, E.; Weber, J.; Fripiat, J. G. *Nouv. J. Chim.* **1978**, *2*, 469.

Table II. Atomic Orbital Populations, Atomic and Ligand Charges q in the Ground States of the Two Complexes $Co(CN)_6^{3-}$ and $Co(CN)_5(OH)^{3-}$ and of the Individual Ligands CN^- and OH^-

$Co(CN)_5(OH)^{3-}$

	3dσ	3dπ	4s	4p	q
Co	1.37	5.73	0.37	−0.07	1.59
	sσ	pσ	total σ	pπ	q
C_{ax}	3.40	1.20		1.76	−0.36
N_{ax}	3.65	1.37		2.37	−0.39
$(CN)_{ax}$			9.62	4.13	−0.75
C_{eq}	3.40	1.20		1.74	−0.34
N_{eq}	3.65	1.37		2.40	−0.42
$(CN)_{eq}$			9.62	4.14	−0.76
O	3.85	1.21		4.00	−1.06
H	0.74	0.00		0.00	0.26
OH			5.80	4.00	−0.80

$Co(CN)_6^{3-}$

	3dσ	3dπ	4s	4p	q
Co	1.63	5.72	0.45	−0.04	1.24
	sσ	pσ	total σ	pπ	q
C	3.37	1.19		1.77	−0.33
N	3.66	1.36		2.36	−0.38
CN			9.58	4.13	−0.71

CN^-

	sσ	pσ	total σ	pπ	q
C	3.87	1.06		1.54	−0.47
N	3.69	1.38		2.46	−0.53
CN			10.00	4.00	−1.00

OH^-

	sσ	pσ	total σ	pπ	q
O	3.91	1.28		4.00	−1.19
H	0.81	0.00		0.00	0.19
OH			6.00	4.00	−1.00

extended Hückel orbitals,[19] where the metal character was found to be closer to 50%.

Figure 1 shows that—both for CN^- and for OH^-—complexation destabilizes the ligand π orbitals more than the ligand σ orbitals. This observation can be rationalized by the interplay of a number of different effects: (i) the approach of six negative ligands tends to destabilize both σ and π orbitals; (ii) the ligand-to-metal donation, accompanying the bonding phenomenon, essentially takes place in the σ orbitals and has an overall stabilizing effect on these orbitals; (iii) the ligand σ orbitals, being directed toward the metal ion, are selectively more stabilized by the positive Co charge. The last two factors tend to decrease the energy of the ligand σ orbitals with respect to the ligand π orbitals.[20]

2. Population Analysis. Table II shows a Mulliken population analysis of the individual ligands and of the two complexes. Because of the rather large basis set used in the present calculations (including some very diffuse functions), the results of a Mulliken population analysis have to be interpreted with some care. Still, the general trends observed in Table II should provide us with a qualitatively correct picture of the bonding phenomenon.

Each CN^- ligand is seen to donate 0.25 to 0.29 electron to the central metal ion; this electron transfer takes place essentially in the σ orbitals, as evidenced by the decrease of the σ(CN) population and by the non-zero population of 3dσ(Co) and 4s(Co) in both complexes. The (weak) π back-bonding, postulated by qualitative MO theory, is reflected by the increased pπ(CN) population and by the decreased number of 3dπ(Co) electrons (5.72 or 5.73, as opposed to 6 in the t_{2g}^6 configuration of the free Co^{3+} ion). The description of the CN^- ligands as strong σ donors and weak π acceptors is essentially identical with the one given by Sano et al.[3]

The OH^- ligand donates 0.20 electron through the σ orbitals; on this basis, one should be inclined to classify OH^- as a weaker σ donor than CN^-. In the π orbitals, no net electron transfer is observed: the pπ(OH) population remains unchanged at 4 electrons (Table II). The absence of any π-electron transfer does not necessarily prevent the hydroxyl ion from being a π-donor ligand. Indeed, also in the simplest classical MO scheme, no net electron transfer can be expected if the bonding and antibonding π orbitals are both fully occupied. Moreover, π-donor or π-acceptor properties are generally inferred from (indirect) spectral data; therefore, this point will be resumed in Section IV.1.

The net charge on the metal is significantly higher in the substituted complex (q = 1.59) than in the parent octahedral compound (q = 1.24). The difference is essentially localized in 3dσ, and the observed decrease in 3dσ population from 1.63 to 1.36 electrons (see Table II) can be accounted for the most part by the reduced σ-donor properties (only 0.20 electron) of OH^-. It is well to stress however that also cyanide ligands appear to be slightly weaker σ donors in the substituted complex than in the octahedral complex. On the other hand, the π-bonding properties of the CN^- ligands are essentially identical in both complexes. In $Co(CN)_5(OH)^{3-}$, no significant differences are apparent between the population patterns of axial and equatorial cyanide ligands.

In order to rationalize the stability of 18-electron compounds, such as $Cr(CO)_6$ or hexacoordinated Co^{3+} complexes, one often invokes an sp^3d^2 hybridization scheme, corresponding to a 1:3:2 population ratio of the valence orbitals 4s, 4p, and 3dσ, respectively. From Table II, this ratio is seen to be roughly 1:0:4, suggesting the inadequacy of the sp^3d^2 hybridization idea. Although the 4s,4p population of ~0.4 electron is certainly not negligible, the hexacoordinated Co^{3+} complexes are apparently closer to the ligand field scheme, where the bonding interactions are essentially carried by the 3d orbitals.

The picture emerging from Table II is quite different from the MS–Xα description of Goursot et al.[7] First of all, it is well to realize that the MS–Xα charges are evaluated by a different procedure, namely by the integration of the charge density over spherical volumes, representing the different atoms. The intersphere charge was fully attributed to the ligands and distributed among them, in each MO, proportionally to their orbital charge. Even by thus assigning the intersphere charge completely to the ligands, the Co charge was found to be negative (−0.80 for $Co(CN)_6^{3-}$ and −0.64 for $Co(CN)_5(OH)^{3-}$). Obviously, it is difficult to compare these numbers directly to our Hartree–Fock results (+1.24 and +1.59, respectively). Still, both calculations agree in predicting that the substituted complex carried less electron density on the Co atom. However, the MS–Xα calculation situates the reduction of the σ donation from the ligands entirely in the 4s(Co) and 4p(Co) orbitals. As a matter of fact, their 3dσ(Co) Xα population *increases* from $Co(CN)_6^{3-}$ to $Co(CN)_5(OH)^{3-}$. Also, the Xα calculation predicts the OH^- ligand to donate 0.14 electron from its π(OH) orbital into 3d(Co); it further suggests that the equatorial CN^- ligands be characterized by π-acceptor properties, somewhat similar to the octahedral ligands, but that the axial CN^- ligand be characterized by π-donor properties!

On the whole, the SCF calculations appear to be more in line with the ligand field picture[11] than the MS–Xα calculations: from Table II, it appears that the role of 4s(Co) and of the 4p(Co) orbitals is rather limited and that the relative σ and π properties of the two ligands are as suggested by semiempirical considerations; moreover, the bonding properties of the inert ligands are not drastically affected by substitution.

3. Density Plots. Figure 2 shows the total density difference Δρ between the $Co(CN)_6^{3-}$ ground state and the individual con-

(19) Alexander, J. J.; Gray, H. B. *Coord. Chem. Rev.* **1967**, *2*, 29.
(20) In the case of the tetragonal complex the large σ–π separation even leads to a positive orbital energy η of the topmost (12e) orbitals. Therefore, Koopmans theory would predict a spontaneous electron loss in this case. This is obviously an artifact of the calculation, which is due to the fact that one studies an isolated trinegative ion. In all actual experimental conditions, this complex ion is stabilized by positive counterions or dipolar solvent molecules. It is well-known[3,21] that inclusion of these additional electrostatic interactions stabilizes all orbitals so as to remove artificially positive η values.
(21) Demuynck, J.; Veillard, A.; Wahlgren, U. *J. Am. Chem. Soc.* **1973**, *95*, 5563.

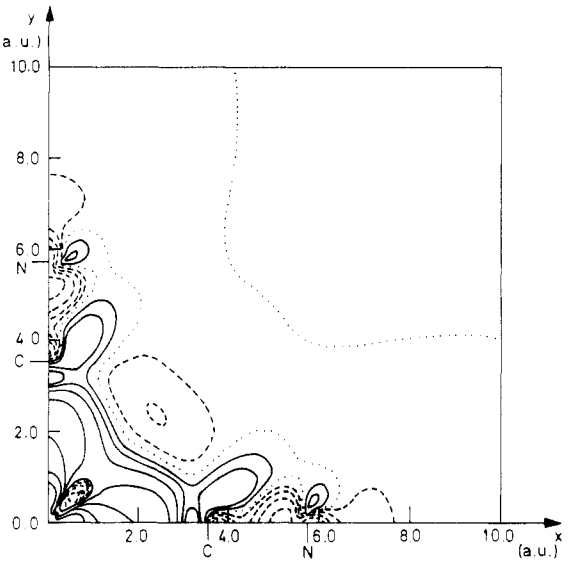

Figure 2. Total density difference plot $\Delta\rho$ = ρ(complex) − ρ(metal–ligand system) for the $^1A_{1g}$ ground state of $Co(CN)_6^{3-}$. The plot describes the electronic density shifts in the *xy* plane upon bond formation; the separated metal–ligand system is considered to be made up of $Co^{3+}(t_{2g}^6; {}^1A_{1g})$ plus six $CN^-(^1\Sigma^+)$ ligands, all noninteracting but kept at the internuclear distances of the complex. Full contours correspond to an electron density increase and dashed contours to an electron density decrease; at the dotted lines, $\Delta\rho$ = 0. The values of the $\Delta\rho$ contours are ±0.0025, ±0.005, ±0.01, ±0.02, ±0.04, ±0.08, and ±0.16 au^{-3}.

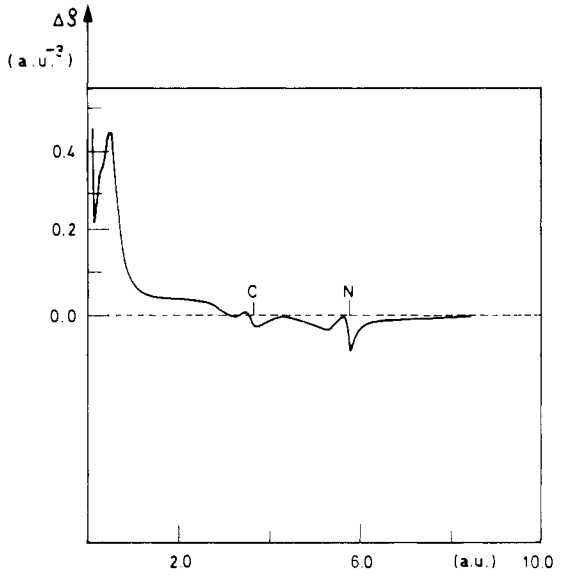

Figure 3. Total density difference $\Delta\rho$ for the $Co(CN)_6^{3-}$ ground state (as in Figure 2) along the *x* axis.

stituents $[Co^{3+}(^1A_{1g};t_{2g}^6) + 6\ CN^-(^1\Sigma^+)]$. The general pattern of population analysis is clearly confirmed: upon bond formation, electron density is withdrawn from the ligands and accumulated on the metal; this is especially obvious in the metal σ orbitals. π back-bonding is evidenced by the density increase in the π zone of the carbon atoms. Although the general features of Figure 2 are similar to Sano's[3] previously published density difference plot, the carbon–nitrogen bonding region appears to be rather different: whereas Sano et al. observed a pronounced polarization of the CN^- ligand (depopulation of N, population of C), Figure 2 is characterized by a density decrease along the entire σ(CN) bond axis, as illustrated more explicitly in Figure 3. Apart from the CN σ-bond weakening Figure 3 also shows a buildup of electronic density in the region between C and Co at around 2 au; the existence of this positive plateau might be thought of as conferring a certain covalency to the metal–ligand bond.

The total density difference plot may be split into partial density difference plots, corresponding to specific irreducible represent-

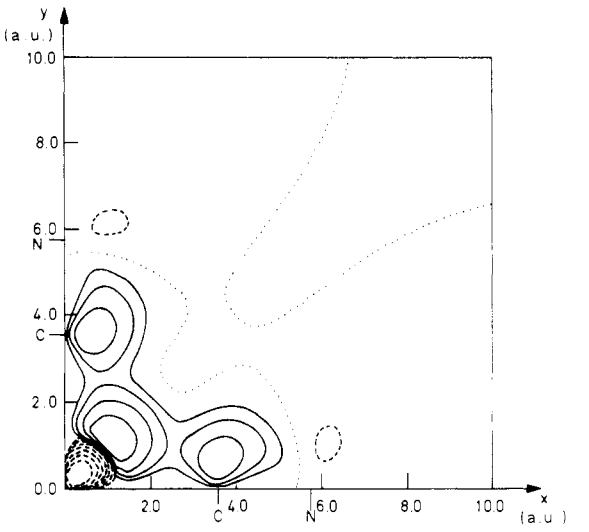

Figure 4. Constituent part of Figure 2, showing only the density differences in the $Co(CN)_6^{3-}$ ground state, due to electronic shifts within the t_{2g} representation $\Delta\rho_\pi$. The values of the $\Delta\rho$ contours are ±0.000 625, ±0.001 25, ±0.0025, ±0.005, ±0.01, ±0.02, ±0.04, and ±0.08 au^{-3}.

ations. Figure 4 gives a detailed description of the t_{2g} density shifts ($\Delta\rho_\pi$), describing the π interactions only; apart from the density increase on carbon, which can be ascribed to back-bonding, one observes an expansion of the 3dπ orbitals. This expansion is a consequence of the σ donation from the ligands: due to the decreased global charge (q = 1.24, vs. 3 in the free metal ion) the occupied 3dπ(Co) valence electrons will tend to expand. This phenomenon had been postulated by Jørgensen in his discussion of the nephelauxetic effect and has been referred to as "central-field covalency";[22] in the same vein, the extension of the $1t_{2g}$(3dπ) orbital onto C can be regarded as an illustration of what has been termed "symmetry-restricted covalency".[22,23]

Similarly, the density shifts within the e_g representation $\Delta\rho_\sigma$ illustrate specifically the σ-electron transfer from the ligand to the metal $3d_{z^2}$ and $3d_{x^2-y^2}$ orbitals.

From $\Delta\rho_\pi$ and $\Delta\rho_\sigma$, it looks as if the classical concepts and the conventional picture of metal–ligand bonding can be maintained without significant modifications.[24] And indeed, if one considers the sum $\Delta\rho_\sigma + \Delta\rho_\pi$, one observes many of the general features of Figure 2. One noticeable exception is the density buildup between C and Co, which was also discussed in connection with Figure 3. Obviously, the "covalent effect" takes place only *partly* within the e_g(dσ) and t_{2g}(dπ) representations: the outer part of the covalent plateau should be associated with the 4s,4p(Co) population in the a_{1g} and t_{1u} representations, thereby constituting a small but striking correction to the d-only description.

Another interesting feature of Figures 2 and 4 can be observed in the π region of the N atoms. Whereas Figure 2 might suggest that the small zone of positive $\Delta\rho$ be due to π back-donation, Figure 4 clearly shows that this is not the case; in fact, the π-electron density of N *decreases* upon bond formation. The positive region in Figure 2 is obviously due to a contraction of other orbitals

(22) Jørgensen, C. K. "Orbitals in Atoms and Molecules"; Academic Press: New York, 1962.

(23) Strictly speaking, the nephelauxetic effect describes the changes from the atomic 3d orbital to the molecular $1t_{2g}$ 3d orbital. Therefore, one should consider a density difference of just those orbitals and not—as in Figure 5—of all orbitals within the t_{2g} representation. Qualitatively, however, the two density difference plots are rather similar and the conclusions in the text remain entirely valid. It should be stressed, however, that Jørgensen's introduction of the nephelauxetic effect was prompted by spectroscopic observations, whereas in the text, the phenomenon is analyzed solely on the basis of the ground-state wavefunction. Therefore, this point will be resumed in Section IV.1.

(24) In ref 11, the π parameter for the Co–CN interaction is listed as 0.39 kK and for Cr–CN as −0.29 kK. These very small values suggest a significant back-bonding, effectively canceling the π interaction between the π-bonding CN orbitals and the metal dπ orbitals.

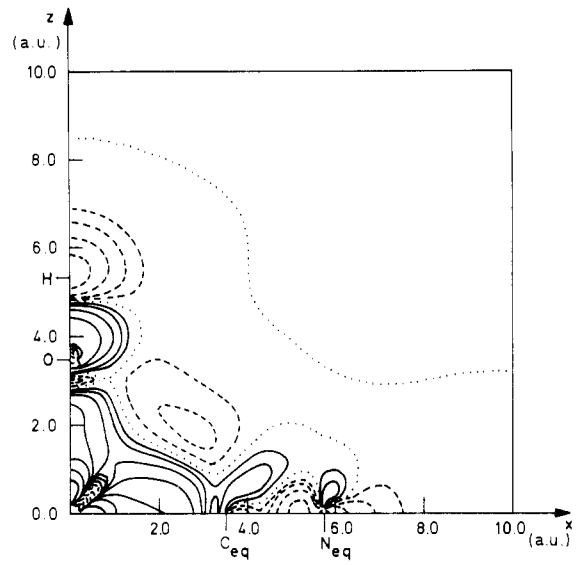

Figure 5. Total density difference $\Delta\rho = \rho(\text{complex}) - \rho(\text{metal–ligand system})$ for the $^1A_1$ ground state of $Co(CN)_5(OH)^{3-}$. The plot describes the density shifts in the xz plane upon bond formation. The contour conventions are as in Figure 2.

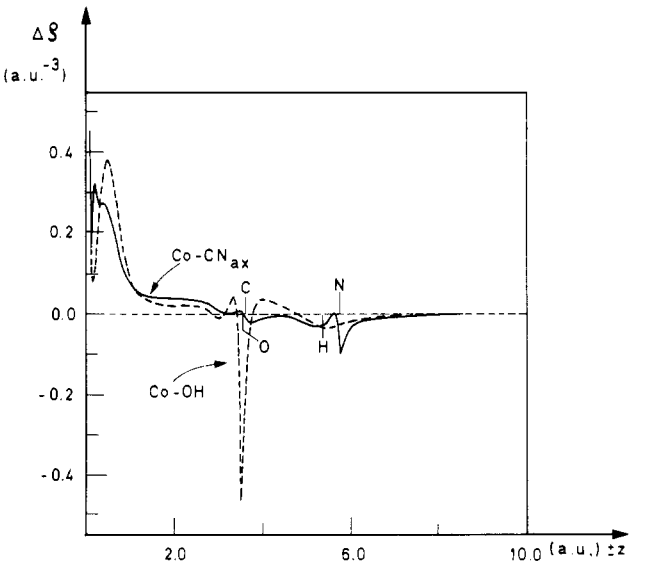

Figure 6. Section along the $\pm z$ axis of the $\Delta\rho$ plots. The full line describes the density shift upon bond formation along the axial Co–CN bond; the dashed line describes the corresponding shift along the Co–OH bond.

(in other representations) following the electron withdrawal associated with the σ donation.

The Co–CN bonds in the substituted complex look qualitatively very similar to the Co–CN bond in the octahedral complex (Figure 2). Apparently, substitution hardly affects the general picture of the inert bonds. In this sense, one of the central hypotheses of ligand field theory, namely ligand additivity, seems to find some ab initio confirmation. A detailed breakdown of the total difference density into σ and π contributions is not possible in the tetragonal complex, since both bonding types are mixed by the low-symmetry field. Only the b_2 representation describes pure $\pi_{\parallel}(CN)_{eq}$ bonds; when the b_2 difference density is calculated in the xy plane of the tetragonal complex, one obtains a plot that is very similar to Figure 4. This result illustrates that the π back-bonding to the equatorial cyanide ligands remains essentially unaffected by the presence of the axial hydroxyl ion.

Figure 5 shows the total density difference plot for $Co(CN)_5(OH)^{3-}$ in the $+xz$ quadrant, containing the hydroxyl ligand. The figure illustrates the σ-donor properties of the OH^- ligand and the population increase in the metal d_{z^2} orbital. The hydroxyl ion is clearly more polarized than the CN^- ligands: electron density is withdrawn from the hydrogen atom and added to the oxygen nucleus under influence of the positive metal ion.

It is not obvious how to make the most relevant comparison between the three different metal–ligand bonds. If the electron density along the bond axes is plotted as in Figure 6, the Co–$(CN)_{ax}$ and the Co–$(CN)_{eq}$ bonds are found to be quite similar to each other and to Figure 3 except for the smaller $\Delta\rho$ value on the Co ion in the substituted complex. The Co–OH bond is found (Figure 6) to be also characterized by a plateau in the bonding region between Co and O, but the surface under the plateau is only about half as large as in the cyanide bonds. This fact is an indication of the weaker σ-bond strength of the hydroxyl ligand; it may be responsible for the experimentally observed OH^- exchange in the thermal substitution reactions. For the two complexes under consideration, there appears to be a relationship between the height of the covalent plateau and the amount of σ donation: ~0.4 e for a cyanide ligand and ~0.2 e for a hydroxyl ligand (Table II).

Although the ab initio results to some extent confirm the classical ligand field ideas,[10,11] the overall picture is somewhat less simple.

IV. Description of the Excited States

1. Total Energies and Energy Splittings. The results for the most important ligand field transitions are shown in Table III and in Figure 7. As usual, the semiempirical ligand field (LF) theory

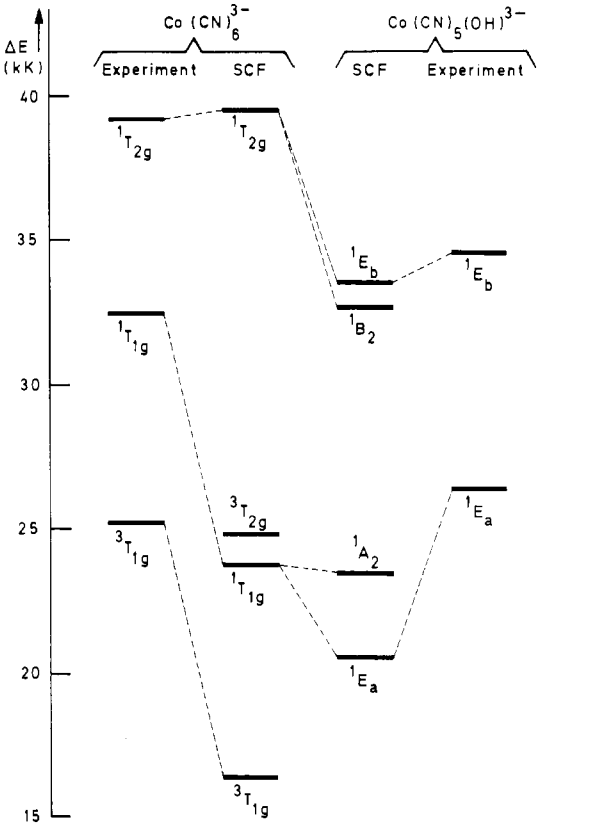

Figure 7. Comparison between the experimental spectra of the two complexes under consideration and the SCF energies. The configurations of the different states are shown in Table III.

adequately reproduces the experimental data even to first order in perturbation theory.[25] The first-order LF expressions are given in Table III. The relevant LF parameters were taken from a detailed comparative study of a number of substituted complexes;[11,24,26] these semiempirical parameters are listed in Table IVa.

(25) The parameter set used in Table III was derived on the basis of a complete ligand field matrix diagonalization. Using this same set in the first-order expressions is obviously not the best way to obtain an optimal fit. The results of the complete diagonalization would reduce the standard deviation by some 800–1000 cm^{-1}.

Table III. Transition Energies (in cm^{-1}) of the Ligand Field Spectrum of $Co(CN)_6^{3-}$ and $Co(CN)_5(OH)^{3-}$ [a]

$Co(CN)_6^{3-}$						$Co(CN)_5(OH)^{3-}$				
			ligand field energies	SCF					ligand field energies	SCF
state	first-order LFT	exptl		this work	Sano[3]	state	first-order LFT	exptl		this work
$^1A_{1g}$	0	0	0	0	0	$^1A_1$	0	0	0	0
$^3T_{1g}(pq \rightarrow p^2 - q^2)$	$10Dq - 3C$	25 200	24 246	16 372	15 165	$^3E_a(xz,yz \rightarrow z^2)$ $^3A_2(xy \rightarrow x^2 - y^2)$	$10Dq - \Delta\sigma + \Delta\pi - 3C + 2B$ $10Dq - 3C$		18 452 24 246	10 074 15 903
$^3T_{2g}(pq \rightarrow r^2)$	$10Dq - 3C + 8B$		27 830	24 779	23 879	$^3B_2(xy \rightarrow z^2)$ $^3E_b(xz,yz \rightarrow x^2 - y^2)$	$10Dq - \Delta\sigma - 3C + 8B$ $10Dq + \Delta\pi - 3C + 6B$		25 290 22 784	16 294 19 527
$^1T_{1g}(pq \rightarrow p^2 - q^2)$	$10Dq - C$	32 500	31 342	23 813	27 895	$^1E_a(xz,yz \rightarrow z^2)$ $^1A_2(xy \rightarrow x^2 - y^2)$	$10Dq - \Delta\sigma + \Delta\pi - C + 4B$ $10Dq - C$	26 400	26 444 31 342	20 598 23 523
$^1T_{2g}(pq \rightarrow r^2)$	$10Dq - C + 16B$	39 200	38 510	39 558	33 755	$^1B_2(xy \rightarrow z^2)$ $^1E_b(xz,yz \rightarrow x^2 - y^2)$	$10Dq - \Delta\sigma - C + 16B$ $10Dq + \Delta\pi - C + 12B$	34 600	35 970 32 568	32 730 33 564

[a] The ligand field (LF) values are first-order results calculated on the basis of the classical ligand field parameters.[11,24,26] For each excited state, the corresponding orbital transition is explicitly specified; for the octahedral complex, *p*, *q*, and *r* each stand for *x*, *y*, and *z*.

Table IV. Ligand Field Parameters[c]

(a) Semiempirical LF Parameters (cm^{-1})[a]

$10Dq = 3\sigma(CN) - 4\pi(CN)$	34890	$\Delta\sigma = \sigma(CN) - \sigma(OH)$	2540
B	448	$\Delta\pi = \pi(CN) - \pi(OH)$	−4150
C	3548		

(b) Theoretical LF Parameters (cm^{-1})[b]

$10Dq'$	27978	$\Delta\sigma'$	6467
B'	956	$\Delta\pi'$	−1564
C'	3989		

[a] Numerical values of the LF Parameters reproducing the experimental t^5e^1 levels. $10Dq$ is the octahedral Co–CN parameter; B and C are the metal Racah parameters. $\Delta\sigma$ and $\Delta\pi$ are the AOM differences (in the σ and π parameters) between the CN^- and OH^- ligands. [b] Numerical values of the LF parameters reproducing the SCF calculated levels (prime symbols). [c] In parts a and b the average error of the fit amounts to about 500 cm^{-1}.

Numerically, the SCF results are somewhat less satisfactory. Rather typically,[1,2] the interconfigurational energy gaps are calculated too small, whereas the intraconfigurational energy gaps are too large. This phenomenon is seen quite clearly in Table IVb, where the numerical SCF results were fitted to the first-order ligand field expressions of Table III, thereby leading to "theoretical" LF parameters (prime symbols). The $10Dq'$(CN) parameter (characteristic of the interconfigurational transitions) is too small, while the Racah B' and C' parameters (characteristic of the splitting within the t^5e^1 configuration) are too large. As a result of the cancellation of both errors, the high-lying $^1T_{2g}$ state is calculated quite close to its observed position. A more detailed analysis of the excitation energies and energy components is given in a separate publication.[27]

An interesting point is the value of the AOM parameters $\Delta\sigma = \sigma(CN) - \sigma(OH)$ and $\Delta\pi = \pi(CN) - \pi(OH)$. The SCF calculations agree with the well-known semiempirical conclusions in that OH^- is found to be a weaker σ donor and a stronger π donor than CN^-. Numerically, however, the ab initio results attribute the main difference between the two ligands to their σ parameters; they suggest less drastic differences between CN^- and OH^- in their π-donor or -acceptor strength. In ligand field theory, $3(\Delta\sigma) - 4(\Delta\pi) = 10Dq(CN) - 10Dq(OH)$; the numerical value of this quantity is found to be of comparable magnitude if calculated from Table IVa (24 000 cm^{-1}) or Table IVb (26 000 cm^{-1}).

The most obvious confirmation of the transferability idea can be found from a comparison of the octahedral $^{1,3}T_{1g}$ states and the tetragonal $^{1,3}A_2$ states, which have identical first-order LF energies and very close lying SCF energies (Table III).

In going from the parameter set of part a of Table IV to that of part b, the sign of the T_{2g} splittings is reversed; this fact can be verified directly from the last two columns of Table III. As shown in Figure 7, the experimental data do not allow one to decide whether $^1B_2$ is above or below ^1E_b. It is well to stress, however, that the CI between ^1E_a and ^1E_b (which is ignored in Tables III and IV) will tend to push the E_b states to higher energy,[28] rendering the SCF order even more probable. As an exploratory step in this direction, a two-configuration CI calculation was carried out for the E_a and E_b states under consideration. The relevant energy shift (stabilizing E_a and destabilizing E_b) was calculated at 1217 cm^{-1}.

As mentioned already in Section III.1, the relative position of the d-type orbitals in the ground state $^1A_1$ is $\eta(6e;d_{xz},d_{yz}) < \eta(1b_2;d_{xy})$. Yet, from the SCF analysis of the excited states, one

(26) Viaene, L.; D'Olieslager, J.; Ceulemans, A.; Vanquickenborne, L. G. *J. Am. Chem. Soc.* **1979**, *101*, 1405.
(27) Vanquickenborne, L. G.; Hyla-Kryspin, I.; Hendrickx, M. In "Quantum Chemistry: The Challenge of Transition Metals and Coordination Chemistry"; Veillard, A., Ed.; D. Reidel: Dordrecht, The Netherlands, 1986.
(28) In the framework of ligand field theory, the E_a states correspond to excitation to z^2 for more than 90%; similarly, in the E_b states, $x^2 - y^2$ is populated for more than 90%, indicating a rather limited configuration interaction.

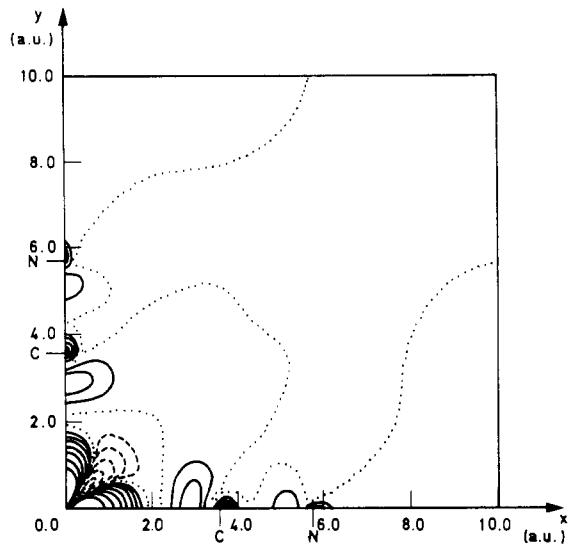

Figure 8. Total density difference plot $\rho(^3T_{1g}) - \rho(^1A_{1g})$ of the octahedral $Co(CN)_6^{3-}$ complex. The plot describes the density shifts (in the xy plane) in going from the ground state to the first excited state of the molecule. The contour conventions are as in Figure 2.

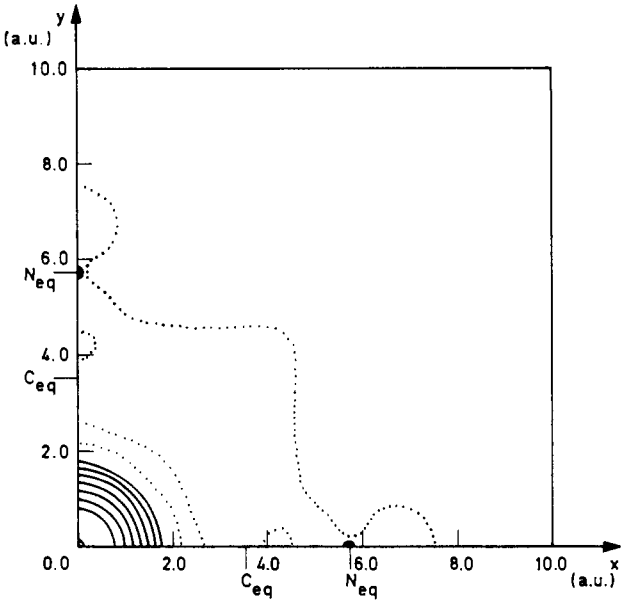

Figure 9. Total density difference plot $\rho(^3E_g) - \rho(^1A_1)$ of the substituted complex. The plot describes the density shifts (in the xy plane) in going from the ground state to the first excited, photoactive state of the molecule. The contour conventions are as in Figure 2.

has to conclude that OH^- is the stronger π donor. The ligand field parameters, being deduced from spectroscopic data, are in agreement with the latter point of view. But the implication of a certain relative sequence of the orbitals in the ground state (which was immediate in LF theory) is obviously invalid in ab initio work. This observation illustrates—in an alternative way—the well-known fact that the meanings of orbital energies are quite different in both theories and that comparisons should only be carried out with utmost care.

A similar remark could be made on the nephelauxetic effect. In Section III.3, it was shown that the ground-state function is characterized by certain properties that might be considered as "nephelauxetic" (Figure 4). Originally, however, the idea of the nephelauxetic effect was introduced by Jørgensen from a study of the LF excited states: the semiempirical Racah parameters B and C, fitting the experimental spectrum of the complex, are in general smaller than the Racah parameters B_0 and C_0, characterizing the free metal ion. In this sense of the word, the nephelauxetic effect can only be calculated from SCF results by comparing the B' and C' values of Table IVb with the B_0' and C_0' values calculated from the SCF results of the free Co^{3+} ion. If one does so, one obtains $B_0' = 1374$ cm^{-1} and $C_0' = 5129$ cm^{-1} or $B'/B_0' = 0.67$ and $C'/C_0' = 0.73$. Rather typically,[1,2] the SCF calculations predict a certain nephelauxetic effect, but quantitatively, the effect is too small; indeed, the semiempirical ratio B/B_0 is known to be approximately 0.5. Obviously, consideration of covalency effects (both of the central-field type and of the symmetry-restricted type) accounts for only part of the nephelauxetic effect. The other part clearly falls outside the scope of SCF calculations and would require the inclusion of configuration interaction.

One final remark should be made regarding the results of Sano et al.[3] The numerical values for the triplet states are quite similar to ours (Table III), and the differences are probably due to the changes in basis set. However, the singlet states calculated by Sano and by us are probably too different to be traceable to a basis set effect. One reason we feel rather confident in our results is the just-mentioned fact that our $^{1,3}T_{1g}$ states (in O_h) and the $^{1,3}A_2$ states (in C_{4v}) are calculated at nearly the same excitation energies. This result is not only predicted by first-order ligand field theory but is also generally observed in monosubstituted complexes (where the experimental band resolution is sufficiently accurate).

2. Density Plots. We will confine our attention to the lowest excited states which are of special importance in discussing the photochemistry of the complexes. Figure 8 shows the density difference plot between the photoactive $^3T_{1g}$ state and the $^1A_{1g}$ ground state of $Co(CN)_6^{3-}$. One observes the depopulation of the d_{xy} zone and the population of $d_{x^2-y^2}$ upon excitation. Simultaneously the σ donation from CN^- is decreased significantly, as

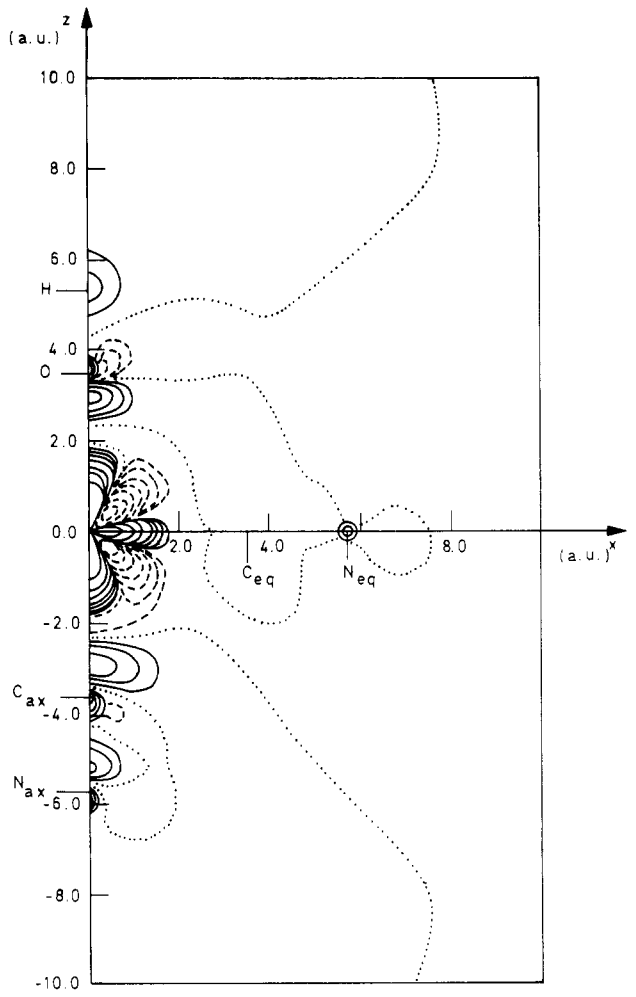

Figure 10. Total density difference plot $\rho(^3E_g) - \rho(^1A_1)$ of the substituted complex. The plot describes the density shifts in the xz plane, in going from the ground state to the first excited, photoactive state of the molecule. The contour conventions are as in Figure 2.

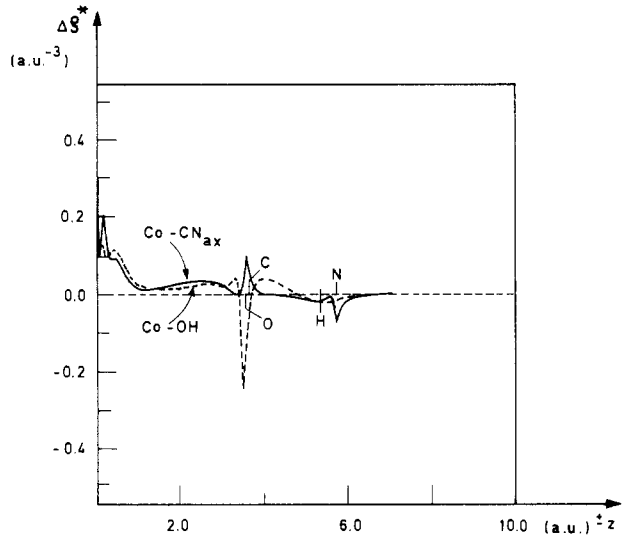

Figure 11. Total density difference plot $\Delta\rho^* = \rho(\text{complex}) - \rho(\text{metal–ligand system})$ for the photoactive ^3E_a state of $Co(CN)_5(OH)^{3-}$ along the $\pm z$ axis. In this case the separated metal–ligand system is considered to be made up of $Co^{3+}[(xy)^2(z^2)^1(xz,yz)^3;{}^3E]$ plus five CN^- ($^1\Sigma^+$) and one OH^- ($^1\Sigma^+$) ligand. The figure describes the electronic shift upon bond formation in the excited state. The full line describes the density shift along the axial Co–CN bond; the dashed line describes the corresponding shift along the Co–OH bond.

evidenced by the positive density contours on the ligands, especially on the carbon atoms: obviously the chemical bond is weaker in the excited state.

Similar plots can be obtained for the photoactive ^3E_a state of the substituted complex, as shown in Figures 9 and 10. Since the excitation in this case corresponds to $xz,yz \rightarrow z^2$, ligand field theory predicts only a small labilizing effect on the equatorial bonds.[11] Figure 9 shows the difference density plot in the xy plane: apart from the population increase on the central metal ion (due to z^2 occupation) no drastic changes can be detected in the metal–ligand interaction zones. Quite to the contrary, the axial bonds (Figure 10) are modified significantly: the decrease of the σ bonding and of the π back-bonding are even more pronounced than in the octahedral case. Obviously, the SCF calculations basically confirm the LF rationalization of the selective (axial) labilization of the metal–ligand bonds.

This conclusion is reinforced by calculating the corresponding density difference plots for the next excited state $^3A_2$. Since the latter corresponds to an $xy \rightarrow x^2 - y^2$ excitation, LF theory predicts only an equatorial labilization from this state. The SCF density plots are in complete agreement with this conclusion: the total density difference $\rho(^3A_2) - \rho(^1A_1)$ in the xy plane is quite similar to Figure 8; in contrast, along the z axis no significant density shifts are taking place.

As for the axial labilization from the photoactive ^3E_a state, a more difficult question remains: which one of the two axial ligands, OH^- or $(CN^-)_{ax}$, is expelled by excitation. Figure 11 shows the density difference upon bond formation in the excited state, for the two bonds Co–OH and Co–$(CN)_{ax}$. In comparison with Figure 6, where the corresponding plots were given for the ground state, one sees that both the σ donation toward the metal and the height of the covalent plateau have decreased in the excited state. This again indicates that both axial bonds are weakened, but from the ab initio point of view, there is no obvious reason why CN^- release should be the dominant photoreaction mode.

V. Conclusion

1. The effect of ligand substitution on the LF spectrum is reasonably well predicted by SCF calculations. The sign of certain energy splittings is sometimes at variance with classical ligand field theory, but the general features of the metal–ligand interactions are found to be as expected from semiempirical considerations: the CN^- ligand behaves as a strong σ donor and a weak π acceptor and the OH^- ligand as a weaker σ donor and as a π donor. This conclusion follows both from the analysis of the SCF excited energies and from the analysis of the density shifts; it does not follow from the relative order of the orbital energies in the ground state.

2. The AOM postulate of ligand additivity is to some extent substantiated by the ab initio calculations. This conclusion follows both from energy and from electron density calculations.

3. In our Hartree–Fock treatment, the bond labilization induced by photoexcitation can be rationalized essentially in the same way as in simple ligand field theory: ^3E_a is characterized by axial labilization, whereas $^3A_2$ is characterized by equatorial labilization.

Acknowledgment. I.H.-K. gratefully acknowledges the award of a scholarship in the framework of an exchange agreement between the Universities of Leuven, Belgium, and Wroclaw, Poland.

Registry No. $Co(CN)_6^{3-}$, 14897-04-2; $Co(CN)_5(OH)^{3-}$, 16893-73-5.

Contribution from the National Bureau of Standards, Gaithersburg, Maryland 20899

Structure Determination by NMR Spectroscopy. Correlation of $|^2J(^{119}Sn,^1H)|$ and the Me–Sn–Me Angle in Methyltin(IV) Compounds

Thomas P. Lockhart*[1a,b] and William F. Manders*[1a]

Received June 12, 1985

New and published tin–carbon ($|^1J(^{119}Sn,^{13}C)|$, $|^1J|$) and tin–hydrogen ($|^2J(^{119}Sn,^1H)|$, $|^2J|$) J coupling data for 25 methyltin(IV) compounds (several in a variety of solvents) have been collected. From a relationship between $|^1J|$ and the Me–Sn–Me angle, θ, described previously, $|^2J|,\theta$ data pairs have been derived. A plot of these data reveals that θ and $|^2J|$ are related by a smooth curve described by θ (deg) = $0.0161|^2J|^2 - 1.32|^2J| + 133.4$; data for most methyltin(IV) compounds lie within 4° of this empirical line. Data for dimethyltin dichloride and dibromide in solvents of varying coordinating ability are described by a somewhat different relationship: θ (deg) = $0.0105|^2J|^2 - 0.799|^2J| + 122.4$. Several applications of the former equation for determining the structures of methyltin(IV) compounds in solution are briefly described, including its use in the assignment of tin coordination number.

NMR spectroscopy is an important tool for investigating molecular structure in solution. The interpretation of chemical shifts and coupling constants, however, is generally based on crystal structure data (X-ray) and is consequently subject to uncertainties